# Investigation of the performance of the oil gas separator depending on the gas content of the pumped liquid. Development of methods for optimizing the geometry of flow-through parts of centrifugal gas separators

IOP Conf. Series: Materials Science and Engineering **589** (2019) 012033 doi:10.1088/1757-899X/589/1/012033

# Investigation of the performance of the oil gas separator depending on the gas content of the pumped liquid. Development of methods for optimizing the geometry of flow-through parts of centrifugal gas separators

**M Ershov[1] and V Lomakin[1,2]**

[1]BMSTU, Moscow, Russian Federation

[2]Email: Lomakin@bmstu.ru

**Annotation**
This article formulates the problems of using oil separators in the current conditions of well operation, as well as research and pilot implementation of innovative oil production technologies. A variant of the improved flow part of the separator was proposed, a mathematical model was written for its further calculation, and the hydrodynamic calculation itself was carried out, the results of which will later be used to study methods for optimizing the geometry of flow parts of centrifugal gas separators.

## Introduction

At the moment, there is a steady tendency to the deterioration of the operating conditions of wells in the fields of the Russian Federation - deposits with favorable geological field parameters are entering a late stage of development, the relative share of oil production from marginal wells with difficultly recoverable reserves is increasing.

Work is underway to intensify the flow from the bottomhole zone and increase oil recovery, with the result that most of the wells were transferred to operating modes with bottomhole pressures of 3–5 MPa. But the growth rate of the average equipment failure time began to decline, and it became clear that most of the ESP wells with the wear resistance group used could no longer provide a significant increase in the time between failures, since they do not correspond to the changed operating conditions [1]. Serial submersible pumping equipment for well operation is often unable to operate in such difficult conditions.

The share of marginal wells in the Russian Federation is about 30-40%, and most of them have complicating factors: high content of free gas, mechanical impurities, corrosion, salt deposition. An acute problem is the introduction of an effective technology for their operation with an average operating time of at least 600 days [2].

In accordance with this, the task of developing, researching and pilot-industrial introduction of innovative technologies for oil production in complicated conditions with the use of submersible pumping systems becomes urgent. New complete equipment with special design of steps, pump and other elements of the installation is necessary.

In oil-producing wells with a high gas content, an increase in the efficiency of centrifugal pumps (ESPs) is achieved by completing them with centrifugal gas separators, in which free gas is drawn from the pumped fluid to the annular space before the pump reaches the pump inlet.

It was established experimentally [3, 4] that the efficiency of a centrifugal gas separator significantly depends on the dispersion of the gas-liquid structure of the pumped fluid. In a real oil well, on reception of a centrifugal gas separator, a bubble flow regime is usually observed, with the diameter of the gas phase bubbles ranging from 80 to 300 μm [5], [6] - [11].

In order to increase the efficiency of the oil production process at low costs, a number of new conceptual equipment was developed at Rimera Group of Companies, including gas separators with interchangeable augers and multiphase modules with a new work concept. The gas separator is considered to be an unreliable element of a pumping unit due to hydroabrasive cutting of the body due to reverse currents that occur if the pump feed is more than half the estimated gas separator feed and the optimum auger feed installed at the inlet [12]. Reverse currents are a trap for mechanical impurities - their concentration is rapidly increasing, and a rotating abrasive ring can cut the casing and other elements of the gas separator. [13] - [16] Traditionally, they try to solve these problems by reducing the angle of the blades at the screw inlet, but this unnecessarily increases the diffusivity flow-through part and reduces the efficiency of the screw. Together with the specialists of RSU NG, the Research and Development Center of the Rimera Group of Companies developed vortex and centrifugal gas separators with replaceable elements of the flow part. It was proposed to reduce the screw diameter in them, keeping the optimal flow path, the inlet angles and the range of components. In addition, it was decided to separate the inlet part of the gas separator with an axial stage and the separation chamber with a special conical sleeve. In the separation chamber, a separation process takes place, and a rotating ring with a partially separated liquid is formed at the periphery. Previously, this ring pressed on the blades of the stage, supplying the gas-liquid mixture, which led to reverse currents and dispersion. Now the ring presses against the fixed axial support in the form of a conical sleeve and a high pressure gradient occurs, due to which efficient gas separation is carried out.

The obvious advantages of the gas separators developed by the Rimera Group for low-cost installations should be attributed to lower power - this saves energy. In addition, the gas separators are ahead of the well-known counterparts for separation properties and wear resistance.

Currently, there are no methods for calculating the separation characteristics of centrifugal gas separators, taking into account the influence of the degree of dispersion of the gas-liquid mixture pumped by the pump. [17] - [20]

The aim of the presented work is a numerical study of the effect of the dispersed gas-liquid mixture structure on the efficiency of the gas separation process in a centrifugal gas separator, calculation of the gas separator performance with different gas contents and the development of methods for improving the geometry of the flow-through part of the equipment.

**Mathematical model**

In this article, we use the model of a multiphase incompressible fluid flow (ρ = const). Numerical simulation is based on solving discrete analogs of the basic hydrodynamic equations.

The calculation is carried out on the basis of a mathematical model of a divided multiphase flow. That is, for each phase, the equations of mass and momentum transfer are solved separately, but the pressure field is the same for all phases.

The mathematical model consists of a set of differential and algebraic equations:

The volume of the i-th phase in each calculated cell is calculated as:

$$V_i = \int_V \alpha_i dV$$

where $\alpha_i$ – is the concentration of the i-th phase in the cell.

The sum of the concentrations of all phases in the cell is one.

$$\sum_{i6}^{n} \alpha_i = 1$$

The equation of conservation of mass (continuity equation):

$$\frac{\partial}{\partial t}\int_V \alpha_i \rho_i dV + \int_A \alpha_i \rho_i \vec{V_i} d\vec{a}$$

where $\rho_i$ – i-th phase density

$\vec{V_i}$ – i-th phase velocity (in the case of turbulent flow modeling by a RANS-type model averaged over time)

The equation for the change in the amount of motion:

$$\frac{\partial}{\partial t}\int_V \alpha_i \rho_i \vec{V_i} dV + \int_A \alpha_i \rho_i \left(\vec{V_i}\vec{V_i}\right) d\vec{a} = -\int_V \alpha_i \nabla p dV +$$

$$+\int_V \alpha_i \rho_i \vec{g} dV + \int_A \left[\alpha_i \left(T_i + T_i^t\right)\right] d\vec{a} + \int_V \overrightarrow{M_i} dV$$

where $\left(\vec{V_i}\vec{V_i}\right)$ – tensor product of the velocity vectors of the i-th phase.

$p$– pressure

$\vec{g}$ – mass intensity vector (in this case, the gravity force is 9.81 m / s2 and the inertial force due to the rotation of the computational domain)

$T_i$ - molecular viscosity stress tensor

$T_i^t$ – turbulent stress tensor

$\vec{M}$ –vector of total intensity of interfacial interaction forces per unit volume, for a vector $\overrightarrow{M_i}$ fair equality:

$$\sum_i \overrightarrow{M_i} = 0$$

Vector $\overrightarrow{M_i}$ characterizes all the forces that separate phases interact with each other.

$$M_i = \sum_{j \neq i}\left(F_{ij}^D + F_{ij}^{VM} + F_{ij}^L + F_{ij}^{TD} + F_{ij}^{WL}\right)$$

$$\overrightarrow{M_i} = \sum_{i \neq j}\left(\overrightarrow{F_{ij}^D} + \overrightarrow{F_{ij}^{VM}} + \overrightarrow{F_{ij}^L} + \overrightarrow{F_{ij}^{TD}} + \overrightarrow{F_{ij}^{WL}}\right)$$

Where

$\overrightarrow{F_{ij}^D}$ – resistance force,

$\overrightarrow{F_{ij}^{VM}}$ – power of the virtual mass

$\overrightarrow{F_{ij}^L}$ – lifting force

$\overrightarrow{F_{ij}^{TD}}$ – turbulent dispersion force

$\overrightarrow{F_{ij}^{WL}}$ – turbulent dispersion force

Power of resistance

In the case of modeling the flow of continuous and dispersed media, the resistance force acting on the dispersed medium I from the side of the continuous medium j is equal to:

$$\overrightarrow{F_{ij}^{D}} = A_D \overrightarrow{V_r}$$

Where

$A_D$ – linearized drag coefficient

$\overrightarrow{V_r} = \overrightarrow{V_j} - \overrightarrow{V_i}$ – relative velocity of one medium relative to another

$$A_D = C_D \frac{1}{2} \rho_C \left|\overrightarrow{V_r}\right| \left( \frac{a_{cd}}{4} \right)$$

Where

$C_D$ – drag coefficient

$\rho_C$ – continuous phase density

$a_{cd}$ – interaction area of the phases (in this case, the member $\frac{a_{cd}}{4}$ is the projected area of the spherical particle on the plane).

The drag coefficient is based on the relation:

$$C_D = f_D C_{D\infty}$$

Where

$C_{D\infty}$ - coefficient of resistance of a single spherical particle moving in an infinite flow

$f_D$ – coefficient taking into account the concentration of particles

$C_{D\infty}$ is out of relationship:

$$C_{D\infty} = \frac{24}{Re_d}\left(1 + 0.15 Re_d^{0.687}\right) \text{ при } Re_d < 1000$$

And

$$C_{D\infty} = 0,44 \text{ при } Re_d > 1000$$

$$Re_d = \frac{\rho_C \left|V_r\right| l}{\mu_C}$$

$l$– characteristic interaction length or bubble size

$\mu_C$ – dynamic viscosity coefficient of continuous medium

Coefficient $f_D$ is the ratio:

$$f_D = {\alpha_C}^{n_D}$$

$\alpha_C$ – continuous phase concentration

$n_D = -8.3$ for spherical particle

Virtual mass

The inertia of the surrounding fluid affects the acceleration of the particle immersed in the fluid. This effect is modeled by adding mass to the dispersed particle.

The force from the virtual mass acting on phase I, moving rapidly with respect to phase j is found as:

$$\overrightarrow{F_{ij}^{VM}} = C_{VM}\rho_C\alpha_C\left(\overrightarrow{a_j} - \overrightarrow{a_i}\right)$$

$\overrightarrow{a_{j,i}}$ – acceleration of jth and ith phase

$C_{VM} = 0,5$ – virtual mass coefficient for a spherical particle

Lift force

In the case where the flow surrounding the dispersed particle is non-uniform or the particle is swirling, it experiences a force perpendicular to the relative velocity.

$$\overrightarrow{F_{ij}^{L}} = C_{Leff}\rho_C\alpha_d\left(\overrightarrow{V_r} \times \left(\nabla \times \overrightarrow{V_c}\right)\right)$$

$\overrightarrow{V_r}$ – relative phase velocity

$\overrightarrow{V_c}$ – continuous phase speed

$\alpha_d$ – dispersed phase concentration

$C_L = 0,25$ – lift force coefficient

Turbulent dispersion force

Additional change in phase concentrations caused by flow turbulence is modeled as the force of turbulent dispersion

$$\overrightarrow{F_{ij}^{TD}} = A_D\overrightarrow{V_{TD}}$$

$A_D$ – drag force coefficient

$\overrightarrow{V_{TD}}$ – relative slip speed

$$\overrightarrow{V_{TD}} = D_{TD}\left(\frac{\nabla\alpha_d}{\alpha_d} - \frac{\nabla\alpha_c}{\alpha_c}\right)$$

$D_{TD} = C_0\dfrac{\nu_c^t}{\sigma_\alpha}I$ – turbulent diffusion tensor

$$C_0 = 1$$

$\nu_c^t$ – turbulent viscosity coefficient kinematic

$\sigma_\alpha$ – turbulentPrandtl number

$I$– unit tensor

$$\sigma_\alpha = \sigma_0\sqrt{1 + C_\beta\xi^2}\,\frac{1+\eta}{b+\eta}$$

$\sigma_0 = 1$ – unmodified turbulent Prandtl number

$C_\beta = 1,8$ – correction factor

$\xi$ – particle sliding velocity related to the speed of turbulent fluctuations

$\eta$ – particle interaction time related to relaxation time

$b$– the ratio of the accelerations of the continuous / dispersed phase

$$b = \frac{1 + C_{VM}}{\frac{\rho_d}{\rho_c} + C_{VM}}$$

$$\eta = \frac{\tau_I}{\tau_R}$$

$\tau_I$ – characteristic time of interaction of a particle and a turbulent vortex

$\tau_R$ – particlerelaxationtime

$$\tau_I = \frac{\tau_T}{\sigma_0} \frac{1}{\sqrt{1 + C_\beta \xi^2}}$$

$$\tau_T = \frac{2}{3} C_\mu \frac{k_c}{\varepsilon_c}$$

$\varepsilon_c$ — *continuous phase turbulence energy dissipation rate*

$$\tau_R = \tau_D \left( 1 + \frac{\rho_c}{\rho_d} C_{VM} \right)$$

$\tau_D = \frac{\rho_d d^2}{18\mu_c}$ –*characteristic time scale for a dispersed particle*

$$\xi = \frac{\left| \overrightarrow{V_r} \right|}{\sqrt{\frac{2}{3} k_c}}$$

$k_c$ – kinetic turbulence energy of the continuous phase

Wall strength

Being located near the solid wall, the gas bubble undergoes an asymmetrical action from the liquid. The force per unit volume that a gas bubble experiences is equal to:

$$\overrightarrow{F_{ij}^{WL}} = -C_{WL} y_w \alpha_D \rho_C \frac{\left| \overrightarrow{V_{r,\tau}} \right|^2}{d_p} \vec{n}$$

Where

$y_w$ – distance from the wall

$\alpha_D$ – dispersed phase concentration

$\rho_C$ – dispersed phase density

$d_p$ – bubble diameter

$C_{WL}$ –coefficient is a function of the distance from the wall and decreasing with increasing distance

$\vec{n}$ – unit normal to the wall at the point closest to the bubble

$\overrightarrow{V_{r,\tau}}$ – tangent to the wall component of the relative velocity

Coefficient $C_{WL}$ is like:

$$C_{WL} = max\left( C_{W1} + \left( \frac{C_{W2}}{y_w} \right) d_p, 0 \right)$$

Coefficients are$C_{W1} = -0{,}01$, $C_{W2}$=0,05. Thus the force caused by the influence of the wall disappears at a distance from the wall equal to the five diameters of the bubble.

**Mathmodelling Results**

To carry out hydrodynamic calculations, the geometry of the flow section of the oil gas separator was constructed.

At the entrance there is a grid, then a screw, which gives additional turbulence to the flow and creates pressure, then the stator is located, straightening the direction of fluid flow. Next is the drum, which discards the fluid to the periphery, and the gas continues to move closer to the axis of the separator due to the distribution of centrifugal force. On a larger diameter, there is one more straightening flow stator, gas is diverted through a channel into the annular space.

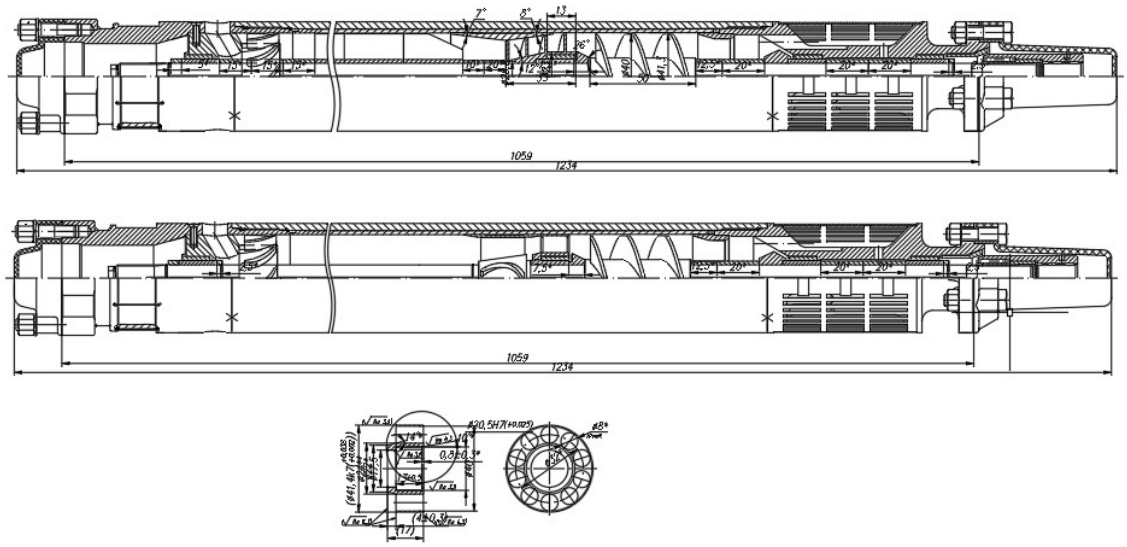


**Pic.1.** Drawing of oil separator

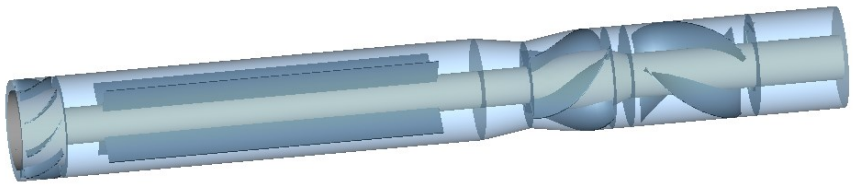

**Pic.2.** 3D model of oil gas separator

For the calculation, the StarCCM software package was used. As the surface mesh, the previously constructed geometry of the flow part was imported.

The following parameters are used as a physical model:

- Multiphase interaction, scale of interaction length 0. 1mm.
- H2O and Air gas (air) are taken as phases.
- Initialliquid / gasdistribution 1/0
- The inlet is set to stagnation at the inlet with a total pressure of 0 Pa and a liquid / gas ratio of 4/1
- At the exit boundary of the fluid, a negative speed is set at 4.5 m / s.
- Atmospheric pressure is set at the gas outlet boundary.

The following parameters were taken as the studied parameters: head, separation coefficient (water fraction at the separator outlet) and power depending on the flow rate.

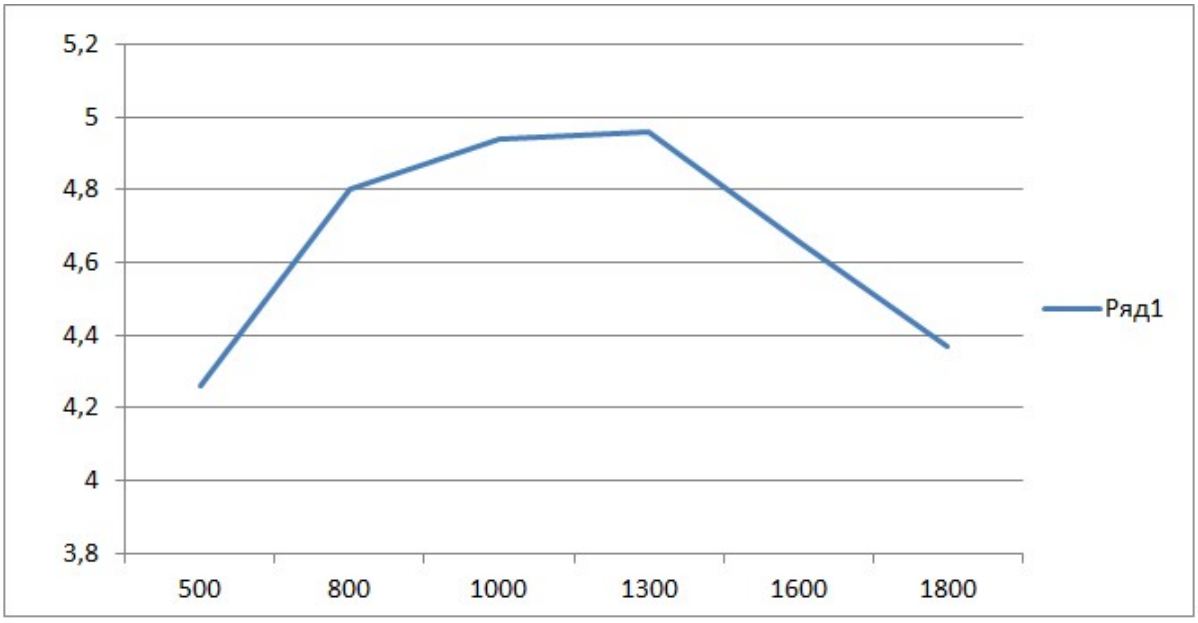


Figure 1. Head (m) versus flow rate (m3 / s)

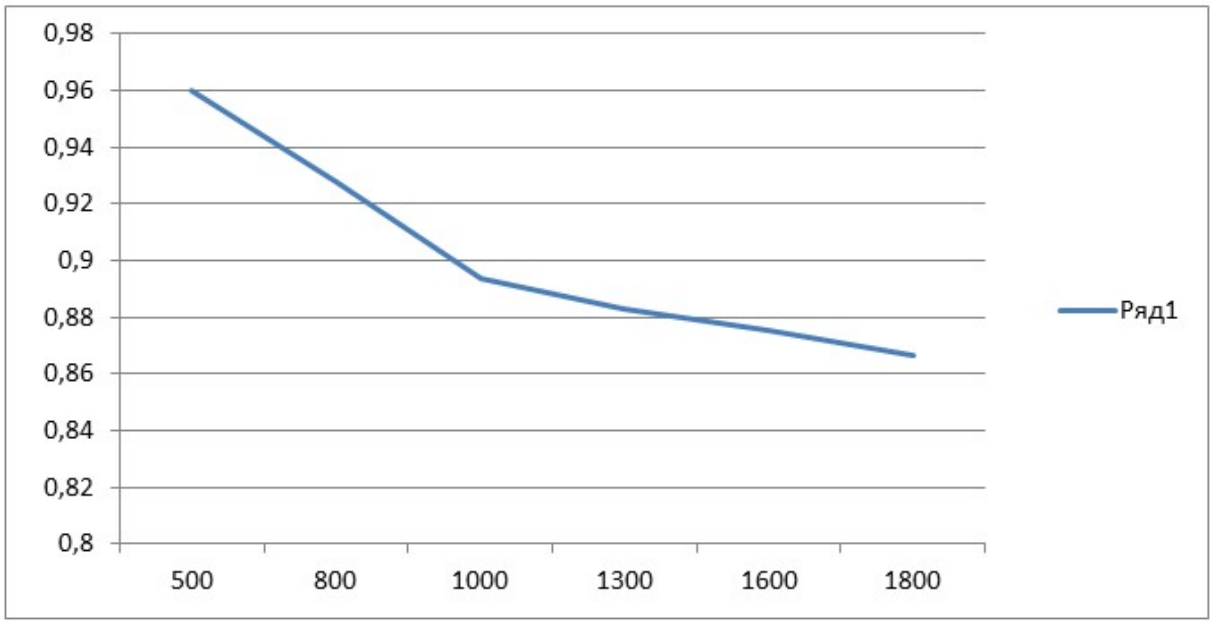


Figure 2. The value of the separation coefficient depending on the flow rate (m3 / s)

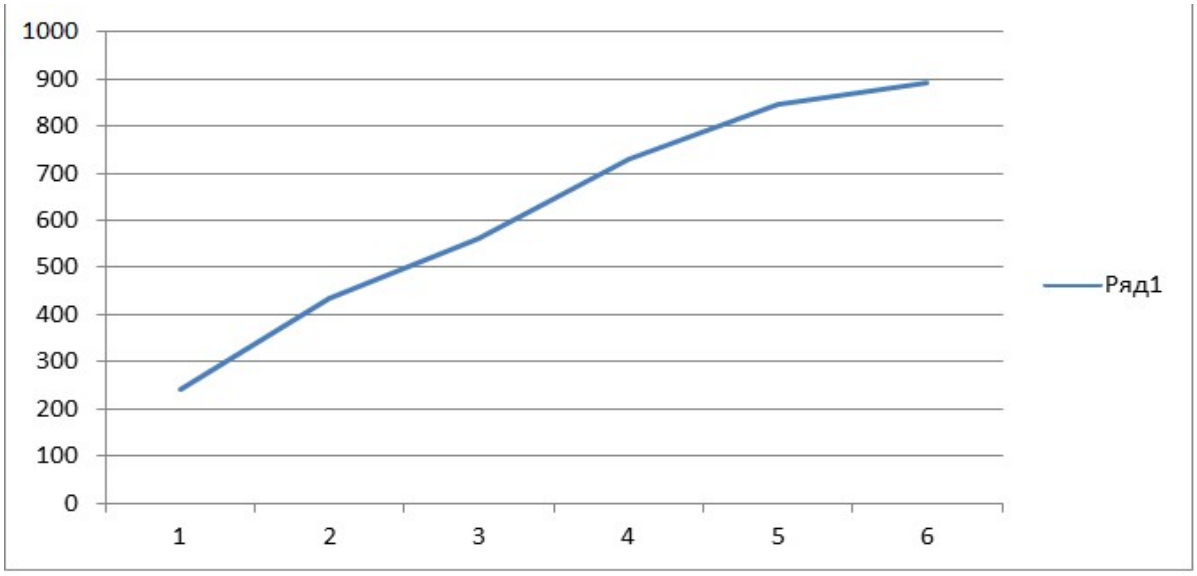


Figure 3. Power value (N * m) depending on the flow rate (m3 / s)

**Findings**

Based on the results, we can draw the following conclusions:

1. Studies of the separator at various values of head from 500 m3 / day to 1800 m3 / day showed that the head graph has a certain peak at a value of 1300 m3 / day, with an increase in flow, the head value begins to fall sharply, with a decrease, the drop occurs smoothly.

2. The value of the separation effect is inversely proportional to the feed, while the graph noticeably changes its rate of decrease approximately at the optimal feed point.

3. The more feed, the more power at the separator shaft. The power at the separator shaft gradually increases in proportion to the increase in the feed value without any jumps.

The obtained characteristics, as well as the constructed geometry of the flow section of the oil gas separator, will be used in future to study methods for optimizing the geometry of the flow sections of the centrifugal gas separators.

**List of references:**

[1] Yakimov S. B. On the prospects of using radially stabilized compression electric centrifugal pumps to improve the efficiency of reservoir operation of the AB group of Samotlor field // Territory "NEFTEGAZ". 2016. No. 6. P. 78-86.

[2] Kosilov D. A. Improving the efficiency of wells ' mechanical Fund management in the current macroeconomic conditions/ Mechanized production // Materials of the specialized section of the Rosneft conference. – M: 2015. – Pp. 8-11.

[3] Iglewski L. V. improving the efficiency of operation of submersible pump-ejector systems for oil: Diss. kand. Techn. sciences'. M., 2002. 216 p.

[4] Dengaev A.V. Improving the efficiency of well operation by submersible centrifugal pumps when pumping gas-liquid mixtures: dis. kand. Techn. sciences'. M., 2005. 212 s

[5] Vasiliev Yu. N., Maksutov R. A., Bashkirov A. I. Experimental study of the structure of oil and gas flow in the fountain well // Oil industry. 1961. No. 4. P. 41-44.

[6] Lomakin V O, Chaburko P S, Kuleshova M S 2017 Multi-criteria Optimization of the Flow of a Centrifugal Pump on Energy and Vibroacoustic Characteristics *Procedia Engineering* **176** pp 476-482

[7] Lomakin V O, Kuleshova M S, Bozh'eva S M 2016 Numerical Modeling of Liquid Flow in a Pump Station *Power Technology and Engineering* **5** pp 324-327
[8] Lomakin V O 2015 Proceedings of 2015 International Conference on Fluid Power and Mechatronics
[9] Lomakin V O, Kuleshova M S, Kraeva E A 2015 Fluid Flow in the Throttle Channel in the Presence of Cavitation*Procedia Engineering* **106** pp 27-35
[10] Shargatov, V.A., Gorkunov, S.V., Il'ichev, A.T. Dynamics of front-like water evaporation phase transition interfaces (2019) Communications in Nonlinear Science and Numerical Simulation, 67, pp. 223-236.
[11] Arefyev, K.Y., Prokhorov, A.N., Saveliev, A.S. Study of the breakup of liquid droplets in the vortex wake behind pylon at high airspeeds (2018) Thermophysics and Aeromechanics, 25 (1), pp. 55-66. DOI: 10.1134/S0869864318010055
[12] Borovsky B. I., Petrov V. I. high-Speed shovel pumps. M., "Mechanical Engineering", 1975.
[13] Gouskov, A.M., Lomakin, V.O., Banin, E.P., Kuleshova, M.S. Minimization of Hemolysis and Improvement of the Hydrodynamic Efficiency of a Circulatory Support Pump by Optimizing the Pump Flowpath (2017) Biomedical Engineering, 51 (4), pp. 229-233. DOI: 10.1007/s10527-017-9720-9
[14] Arefyev, K.Y., Voronetsky, A.V., Suchkov, S.A., Ilchenko, M.A. Computational and experimental study of the two-phase mixing in gas-dynamic ignition system (2017) Thermophysics and Aeromechanics, 24 (2), pp. 225-237. DOI: 10.1134/S086986431702007X
[15] Lomakin, V.O., Kuleshovav, M.S., Bozh'eva, S.M. Numerical Modeling of Liquid Flow in a Pump Station (2016) Power Technology and Engineering, 49 (5), pp. 324-327. DOI: 10.1007/s10749-016-0623-9
[16] Arefyev, K.Y., Voronetsky, A.V. Modelling of the process of fragmentation and vaporization of non-reacting liquid droplets in high-enthalpy gas flows (2015) Thermophysics and Aeromechanics, 22 (5), pp. 585-596. DOI: 10.1134/S0869864315050078
[17] Belov, P.A., Kobets, L.P., Borodulin, A.S. Impregnation kinetics of fibers with liquids: Simulation within the generalization of Navier-Stokes equations (2014) Inorganic Materials: Applied Research, 5 (4), pp. 403-406. DOI: 10.1134/S2075113314040182
[18] Loginov V. F. Compression pumps for oil production in complicated conditions.// Oilandgasjournal. 2016, № 6. С. 54-56.
[19] D. C. Wilcox (1994). "Turbulence modeling for CFD" // DCW Industries, Inc., 460 pages.
[20] Aref'Ev, K.Yu., Voronetskii, A.V., Il'Chenko, M.A. Dynamic characteristics of a resonant gas-dynamic system for ignition of a fuel mixture (2013) Combustion, Explosion and Shock Waves, 49 (6), pp. 657-661. DOI: 10.1134/S0010508213060038